Received: 4 January 2022 | Revised: 28 July 2022 | Accepted: 4 August 2022

DOI: 10.1111/cas.15533

ORIGINAL ARTICLE

Cancer Science WILEY

DDR1 functions as an immune negative factor in colorectal cancer by regulating tumor-infiltrating T cells through IL-18

Xiaofan Duan[1,2] | Xiaoxiao Xu[1,2] | Yumei Zhang[1,2] | Yuan Gao[1,2] | Jiuli Zhou[1] | Jin Li[1]

[1]Department of Oncology, Shanghai East Hospital, Tongji University School of Medicine, Shanghai, China

[2]Tongji University School of Medicine, Shanghai, China

Correspondence
Jin Li and Jiuli Zhou, Department of Oncology, Shanghai East Hospital, Tongji University School of Medicine, 1800 Yuntai Road, Pudong District, Shanghai 200123, China.
Emails: lijin@csco.org.cn; 1610701@tongji.edu.cn

Funding information
National Natural Science Foundation of China, Grant/Award Number: 81772561; Shanghai Sailing Program, Grant/Award Number: 20YF1453300; Top-level Clinical Discipline Project of Shanghai Pudong, Grant/Award Number: PWYgf2021-07

Abstract

Immunotherapies represented by programmed cell death protein 1/programmed cell death ligand 1 (PD-1/PD-L1) immune checkpoint inhibitors have made great progress in the field of anticancer treatment, but most colorectal cancer patients do not benefit from immunotherapy. Discoidin domain receptor 1 (DDR1), a tyrosine kinase receptor, is activated by collagen binding and overexpressed in various malignancies. However, the role of DDR1 in colorectal cancer and immunoregulation remains unclear. In this study, we found DDR1 is highly expressed in colorectal cancer tissues and negatively associated with patient survival. We demonstrated that DDR1 promotes colorectal tumor growth only in vivo. Mechanistically, DDR1 is a negative immunomodulator in colorectal cancer and is involved in low infiltration of $CD4^+$ and $CD8^+$ T cells by inhibiting IL-18 synthesis. We also reported that DDR1 enhances the expression of PD-L1 through activating the c-Jun amino terminal kinase (JNK) signaling pathway. In conclusion, our findings elucidate the immunosuppressive role of DDR1 in colorectal cancer, which may represent a novel target to enhance the efficacy of immunotherapy in colorectal cancer.

KEYWORDS
colorectal cancer, DDR1, IL-18, PD-L1, tumor-infiltrating T cell

1 | INTRODUCTION

Globally, CRC is the third most diagnosed malignancy and the second leading cause of cancer death.[1] In the past decade, following the initial success of melanoma treatment, immunotherapy has rapidly become the mainstay of treatment for a variety of solid cancers, including a subset of colorectal cancer that are mismatch repair deficient (dMMR).[2,3] But this proportion of patients is small and most patients cannot benefit from immunotherapy. Moreover, studies have shown that tumor tissues that do not respond to immunotherapy often lack immune cell infiltration.[4–6] Therefore, it is critical to understand the mechanisms responsible for "cold" immune tumors to boost antitumor immunity.

Discoidin domain receptor 1 is a poorly characterized receptor tyrosine kinase (RTK) that binds to collagens, which are the major components of the extracellular matrix. DDR1 functions as a central

Abbreviations: CRC, colorectal cancer; CTLA-4, cytotoxic T lymphocyte-associated antigen-4; DDR1, Discoidin domain receptor 1; IFN-γ, interferon-γ; IL-18, Interleukin-18; JNK, c-Jun amino terminal kinase; PBMC, peripheral blood mononuclear cell; siRNA, small interfering RNA; TIL, tumor-infiltrating lymphocyte.

Xiaofan Duan and Xiaoxiao Xu have contributed equally to this work.

extracellular matrix sensor to regulate cell adhesion.[7] DDR1 can cross-talk with several transmembrane receptors, including Notch and TGF-β receptors, and influence their signaling upon collagen stimulation.[8] DDR1 also promotes cell proliferation, motility, and invasion, depending on the tumor type and the nature of the microenvironment.[8,9] In colorectal cancer, DDR1 promotes cell survival through the Ras/Raf/MAPK pathways under genotoxic stress and supports the metastatic process through Wnt/β-catenin-dependent, as well as BCR-dependent and PEAK1-dependent, mechanisms.[10,11] It has also been found that DDR1 overexpression can induce colorectal cancer cell invasion through the upregulation of MMP-2.[12] Nevertheless, there has been no relevant report on the immune regulation of DDR1 in CRC.

IL-18, a member of the IL-1 cytokine family, is similar to IL-1β for being processed by caspase 1 to an 18 kDa-biologically active mature form and mediates inflammation downstream of the NLRP3 and NLRP1 inflammasomes.[13,14] In the body, IL-18 is constitutively expressed by several cell types, including macrophages and intestinal epithelial cells. IL-18 promotes the enhancement of CD4 and CD8 cells proliferation and secretion of various cytokines.[15]

However, a connection between DDR1 and the infiltration of immune cells in colorectal cancer has not been established. Here, we report that DDR1 promotes colorectal cancer progression through the enhancement of the immunosuppressive microenvironment, and its mechanism of inhibiting immune cell infiltration is partially mediated by IL-18 and PD-L1. Furthermore, we also show that DDR1 regulates PD-L1 expression through the JNK/c-Jun pathway in CRC.

2 | MATERIALS AND METHODS

2.1 | Cell cultures

Human CRC cell lines (HCT116, HCT8, SW480, LoVo, DLD-1 and RKO) were purchased from the Chinese Academy of Sciences in Shanghai. Mouse CRC cell line MC38 was obtained from Southern Medical University in Guangzhou, China. CRC cells were cultured in DMEM (Gibco) that was supplemented with 10% FBS (Gibco), 100 U/ml penicillin and 100 μg/ml streptomycin, and were maintained in the 5% CO_2 incubator at 37°C. Collagen I (Sigma) was coated on culture plates to stimulate DDR1 (8 μg/cm^2) as previously described.[8]

2.2 | Plasmids, lentivirus infection, and transfection

Cells at 80% density were transfected with siRNAs (Transheep) using RFect reagent (BIOG Nucleic Acid Quick Swab Kit, China) and plasmid (Transheep) using Lipofectamine 3000 (Invitrogen). The target sequences for DDR1 siRNA and IL-18 siRNA sequences are listed in Table S1. After 24 h or 48 h incubation, the cells were collected for subsequent experiments. Lentivirus CMV (pTSB011104/Puro) containing DDR1 overexpression plasmids and lentivirus CMV (pTSB201131/Puro) containing IL-18 overexpression plasmids were purchased from the Transheep company. For the infection of lentivirus-based constructs, cells at 80% confluency were incubated for 24 h in medium containing concentrated viral particles and polybrene (Sigma-Aldrich). The transfected cells were allowed to grow for another 2 days and then selected with puromycin (Sigma-Aldrich) for 1 week. The transfection efficiency was validated by qRT-PCR or western blot.

2.3 | Establishment of DDR1 knockout cell line

To knockout DDR1 in SW480 cells, gene editing was performed using the CRISPR/Cas9 system. Oligonucleotides with *Bsm*B1 restriction sites for guide RNAs were synthesized and cloned into LentiCRISPRv2 together with the puromycin selection marker by Transheep. The sequences of the cloned plasmids that were extracted from numerous selected colonies were confirmed by Transheep. SW480 cells were transfected with LentiCRISPRv2-single guide RNA (sgRNA) DDR1 using Lipofectamine 3000, according to the manufacturer's protocol. Two sgRNAs, DDR1-6-156/rev and DDR1-6-183/fw were simultaneously transfected into cells to knock out DDR1 from two different sites. The two sgRNA sequences of DDR1 were: DDR1-6-156/rev:5′-GTAACGCAGCCGGTAGCTCC-3′; DDR1-6-183/fw: 5′-CTACCGGCTGCGTTACTCCC-3′. The cells were cultured with increasing concentrations of puromycin for 2 weeks, starting at 3 days post-transfection. After routine digestion, the cells were separated using flow cytometry and inoculated into 96-well plates. Single cell clones were expanded and evaluated for gene-specific knockout through immunoblot analysis. DNA sequencing technology was used to confirm the purity of a single clone of DDR1-KO SW480 cells, shown in Figure S1.

2.4 | Proliferation

Cell proliferation assay was tested by 5-ethynyl-2′-deoxyuridine (EdU) Cell Proliferation Assay Kit (BBI Life Sciences). Cells seeded into a 24-well plate in triplicates were manipulated according to the manufacturer's instructions and then photographed using a fluorescence microscope. Red fluorescence indicated that the cells were in a proliferative state, and the number was counted and analyzed.

2.5 | Western blot

Total protein was extracted after lysing the cells with RIPA lysis buffer containing protease inhibitor cocktail. Proteins were separated using SDS-PAGE and transferred to PVDF membranes. Membranes were then blocked with 5% BSA and incubated with primary antibodies. After that, membranes were washed and incubated with HRP-conjugated secondary antibodies. Finally, the protein bands were

visualized using an ECL detection reagent (Millipore). The primary antibodies used are listed in Table S2. Primary antibodies were detected using goat polyclonal rabbit (WELLBIO).

2.6 | Quantitative real-time PCR

Total RNA was extracted using TRIzol (Invitrogen). The cDNA was reverse transcribed according to the manufacturer's instructions. Quantitative real-time PCR (qRT-PCR) was then performed using SYBR Green, and GAPDH was used as an internal control. Relative expression levels were determined using the $2^{-\Delta\Delta C_t}$ method. Primers used are listed in Table S3.

2.7 | Syngeneic mouse tumor model

All mice were housed and treated in accordance with protocols approved by the Animal Care and Use Committee of laboratory animal research center, Tongji University (TJBB04521101). MC38 cells (1.8×10^6 cells for each injection, with 200 ul phosphate-buffered saline resuspension) were injected subcutaneously into 6-week-old female C57bL/6 mice. The length (L) and width (W) of the tumors were measured using an external caliper and the volume (V) of each tumor was calculated according to the equation $[V = (L\times W^2)\times 0.5]$. The mice were euthanized using carbon dioxide asphyxiation. Tumors were excised, weighed, and subjected to immunohistochemistry (IHC), WB, or immune cell profile analysis.

2.8 | Immunohistochemistry (IHC)

Paraffin-embedded slides were deparaffinized, rehydrated and treated with 1×EDTA or citrate at 98°C for 10 min for antigen retrieval. The slides were further incubated in 3% H_2O_2 solution to block endogenous peroxidase. After blocking with 3% BSA, tissues were incubated with primary antibodies against PD-L1 (Proteintech, #14-5983-82), PD-1 (CST, #84651), DDR1 (CST, #5583), CD4 (Abcam, #ab183685) and CD8α (CST, #989941) overnight at 4°C. After rinsing with PBS, the slides were incubated with biotin-conjugated secondary antibody, washed, and incubated with HRP-conjugated streptavidin. The slides were counterstained with hematoxylin. Stained areas were calculated using ImageJ software and statistically analyzed.

2.9 | Cell isolation

Blood samples were collected from healthy donors. PBMCs were isolated with Ficoll–Hypaque (GE Life Sciences) by density gradient centrifugation within 2 h of sample collection. Total $CD8^+$ T cells were purified from PBMCs by negative selection (BioLegend). For the mouse cell isolation, after careful removal of the mouse tumor tissue, portions were minced into 2 mm pieces. Using the Mouse Tumor Dissociation Kit (Miltenyi Biotec Inc.), these tissues were further dissociated into single cells by combining mechanical dissociation and enzymatic degradation of the extracellular matrix. Immune cells were enriched using a discontinuous Percoll (GE Life Sciences) gradient.

2.10 | Co-culture

$CD8^+$ T cells were sorted and co-cultured with SW480 cells in 6-well plates at a ratio of 10:1. Cells were stimulated with αCD3/CD28 (IBA Lifesciences). After 48 h, T cells were collected to determine the cytokine production. Before that, Leukocyte Activation Cocktail (BD) was added and sustained for 8–10 h to block IFN-γ release. To verify the effect of IL-18, rIL-18 (Absin), control IgG (R&D) and IL-18 neutralizing antibody (R&D) were added in a co-culture system for 24 h.

2.11 | Flow cytometry analysis

For multicolor flow cytometry immunophenotypic analysis, cells were stained with the indicated antibodies and analyzed on a CytoFLEX (Beckman Coulter). The flow cytometric profiles were analyzed using counting 20,000–50,000 events using the CytoFLEX software. Information on antibodies is presented in Table S4 and Section 2 and gating strategies for immunophenotyping shown in Figure S2.

2.12 | Enzyme-linked immunosorbent assay

Cells were conditioned for 48 h in serum-free medium. The medium was collected and centrifuged at 300x g for 5 min to remove particles. IL-18 production in the supernatant of SW480 and HCT116 were assessed by enzyme-linked immunosorbent assay (ELISA) using a commercially available ELISA kit (Abcam) according to the manufacturer's recommendations.

2.13 | Statistical analysis

Each experiment was done at least three times, and data are presented as the mean ± SD. All data were analyzed using GraphPad Prism software (version 8.0.1). The comparison between the two groups of values was performed by t-test and one-way analysis of variance (ANOVA) followed by Tukey's multiple comparison test, which was used for more than two groups. A value of $p<0.005$ was considered as a significant difference. In figures, $^*p<0.05$, $^{**}p<0.01$, $^{***}p<0.001$ and $^{****}p<0.0001$.

3 | RESULTS

3.1 | DDR1 expression leads to a poor prognosis in CRC patients, but may not be primarily through promoting tumor cell proliferation

To evaluate DDR1 expression on CRC, we examined the RNA-seq data from multiple malignancies in The Cancer Genome Atlas (TCGA). We found that DDR1 is highly expressed in CRC tissues compared with the adjacent normal tissues (Figure 1A). To further determine the effects and the clinical significance of DDR1, we analyzed the relationship between the expression level of DDR1 and disease-free survival (DFS) in patients with CRC using the PrognoScan database. Notably, we found that higher DDR1 expression positively correlated with poorer DFS (Figure 1B). These results indicated that a high level of DDR1 is a potential risk factor to poor prognosis in patients with CRC.

To directly determine the role of DDR1 in CRC, we first examined the expression of DDR1 in various CRC cell lines. DDR1 was highly expressed in SW480, LoVo, and HCT116 cells, but expressed at relatively low levels in RKO and HCT8 cells (Figure 1C). Then we constructed four independent siRNAs and verified their knockdown efficacy in SW480, HCT116, and MC38 cells (Figure 1D). We selected siRNA-1 for validation at the mRNA level in SW480, HCT116, and MC38 cells (Figure 1E). We also constructed cell lines with DDR1 overexpression using a lentiviral-mediated method (Figure 1F,G). Next, we detected the effect of DDR1 on the proliferative capability in SW480, HCT116, and MC38 cells. However, after overexpression of DDR1, the proportion of cells in the proliferative phase was slightly increased only in HCT116 cells. No significant difference was observed in other cell lines (Figure 1H–K), indicating that DDR1 may not be a direct regulator of CRC cell growth.

3.2 | DDR1 promotes colorectal tumor growth in vivo and suppresses the infiltration of T cells

We sought to test the role of DDR1 on tumor progression in fully immunized mice. We used DDR1-OE MC38 cells to establish a subcutaneous CRC xenograft model in C57bL/6 mice ($n = 7$/group). The tumor volume was monitored. Cells overexpressing DDR1 formed much bigger tumors compared with the control group (Figure 2A–C). We considered whether immunity was involved in this difference. To determine whether DDR1 modulates the tumor immune environment, we analyzed the immune cell profile regulated by DDR1 from xenografts. Flow cytometry analysis showed that $CD4^+$ T cells ($CD45^+CD3^+CD4^+$) and $CD8^+$ T cells ($CD45^+CD3^+CD8a^+$) that infiltrated the tumors were significantly lower in the DDR1-OE group than in the scramble controls (Figure 2D–G).

To further validate the above results, we collected mouse tumor tissues for IHC staining. First, we stained DDR1 and confirmed its high expression (Figure 2H,I). Then, we stained CD4 and CD8a (Figure 2J–M) and reached a conclusion consistent with the flow cytometry results. It was further confirmed that DDR1 overexpression inhibited the infiltration of $CD4^+$ T cells and $CD8^+$ T cells in the tumor microenvironment.

3.3 | DDR1 affects IFN-γ secretion of $CD8^+$ T cells co-cultured with CRC cells in vitro

The activated $CD8^+$ T cells utilize two main pathways for killing their target cells: granule exocytosis and Fas ligand-mediated apoptosis induction. $CD8^+$ T cells also release IFN-γ and tumor necrosis factor α (TNF-α) to induce cytotoxicity in the cancer cells.[16] Therefore, we compared the functional differences in IFN-γ secretion by $CD8^+$ T cells after co-culture with SW480 cells that expressed different levels of DDR1. A DDR1-KO cell line was established using CRISPR/Cas9 technology (Figure 3A). DDR1-OE cell lines were constructed as described previously (Figure 3D). The flow cytometry (FCM) results indicated that DDR1-KO could increase IFN-γ synthesis in $CD8^+$ T cells (Figure 3B,C), whereas DDR1-OE suppressed its synthesis (Figure 3E,F). This suggests that DDR1 not only inhibits the infiltration of T cells, but also inhibits the function of $CD8^+$ T cells.

3.4 | DDR1 affects the synthesis level of IL-18

Interleukins and related cytokines serve as a means of communication between adaptive immune cells and nonimmune cells and tissues.[17] ILs can nurture an environment favoring cancer growth and are essential to generate tumor-specific immune responses.[17,18] To further elucidate the underlying mechanisms in which DDR1 affects immunity, we screened the expression of several ILs and cytokines that may be relevant for immune cell infiltration (Figure S3). Among these

FIGURE 1 DDR1 overexpression negatively correlates with prognosis in CRC, whereas DDR1 does not affect CRC cells proliferation in vitro. (A) DDR1 mRNA levels are increased in CRC samples in The Cancer Genome Atlas (TCGA) database. The red column describes tumor tissues (T) and the black column describes normal tissues (N). (B) DDR1 is associated with poor survival of CRC patients in the PrognoScan database. Disease-free survival (DFS) curves for patients with CRC by DDR1 expression (n [high] = 151, n [[ow] = 75); DFS survival curves for patients with CRC by DDR1 expression (n [high] = 94, n [low] = 51). (C) Expression levels of DDR1 in various CRC cell lines were detected. (D) Four independent siRNAs for DDR1 knockdown were validated in SW480, HCT116, and MC38 cells. (E) The level of DDR1 depletion upon siRNA-1 transfection was assessed by qRT-PCR. (F, G) CRC cell lines with stable overexpression of DDR1 were established. (H–K) Cell lines stablished in (D) and (F) were used for proliferation assays. Fluorescence immunostaining showed nuclei (blue) and EdU (red). Data were expressed as the mean ± SD of three independent experiments. $^*p < 0.05$; $^{***}p < 0.001$; $^{****}p < 0.0001$ (t-test).

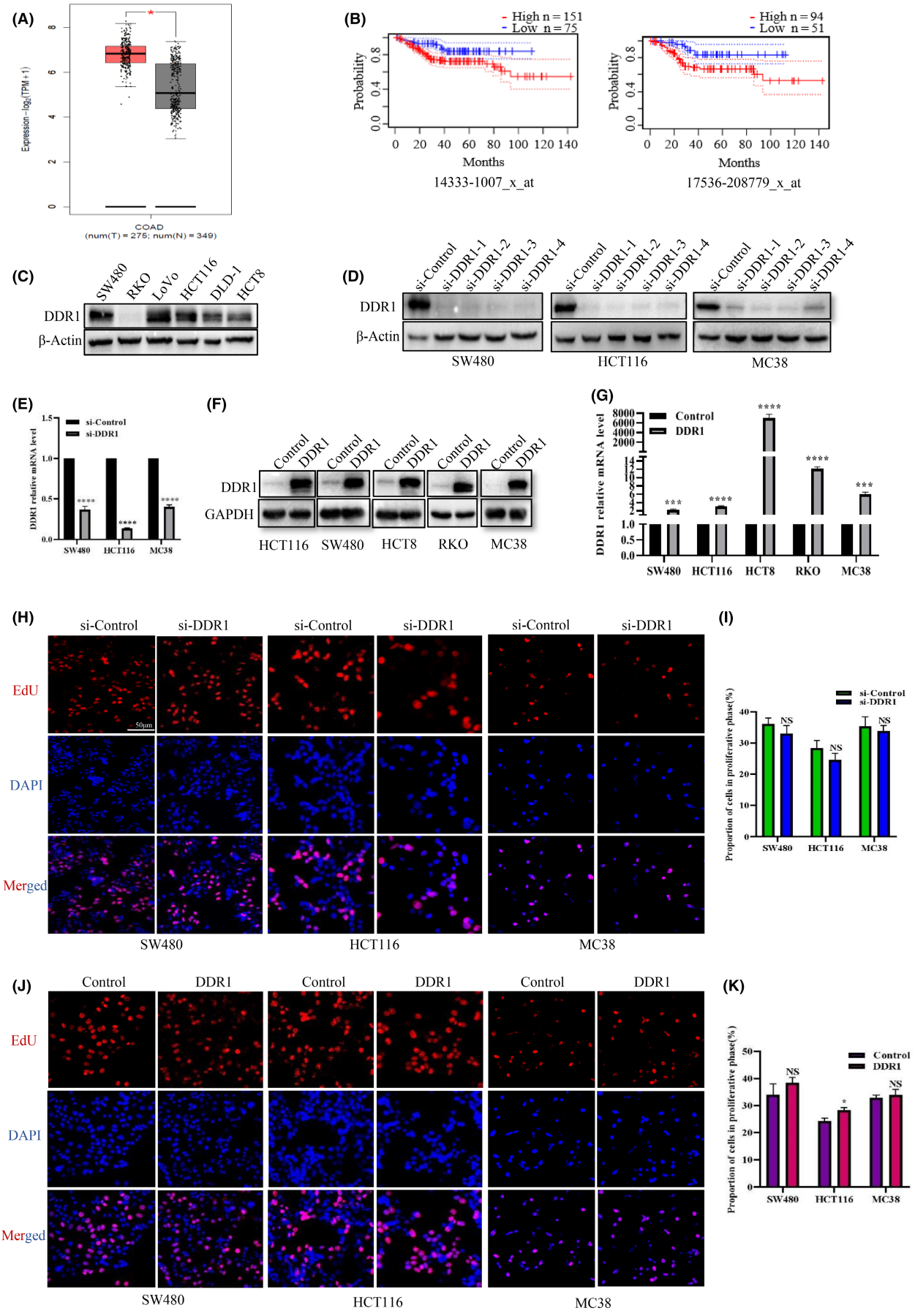
(A)
Expression −log2(TPM+1)
COAD
(num(T) = 275; num(N) = 349)
(B)
High n = 151
Low n = 75
Probability
Months
14333-1007_x_at
High n = 94
Low n = 51
17536-208779_x_at
(C)
SW480 RKO LoVo HCT116 DLD-1 HCT8
DDR1
β-Actin
(D)
si-Control si-DDR1-1 si-DDR1-2 si-DDR1-3 si-DDR1-4
DDR1
β-Actin
SW480 HCT116 MC38
(E)
si-Control
si-DDR1
DDR1 relative mRNA level
SW480 HCT116 MC38
(F)
Control DDR1
DDR1
GAPDH
HCT116 SW480 HCT8 RKO MC38
(G)
Control
DDR1
DDR1 relative mRNA level
SW480 HCT116 HCT8 RKO MC38
(H)
si-Control si-DDR1
EdU
DAPI
Merged
50μm
SW480 HCT116 MC38
(I)
si-Control
si-DDR1
Proportion of cells in proliferative phase(%)
NS
SW480 HCT116 MC38
(J)
Control DDR1
EdU
DAPI
Merged
SW480 HCT116 MC38
(K)
Control
DDR1
Proportion of cells in proliferative phase(%)
NS
SW480 HCT116 MC38

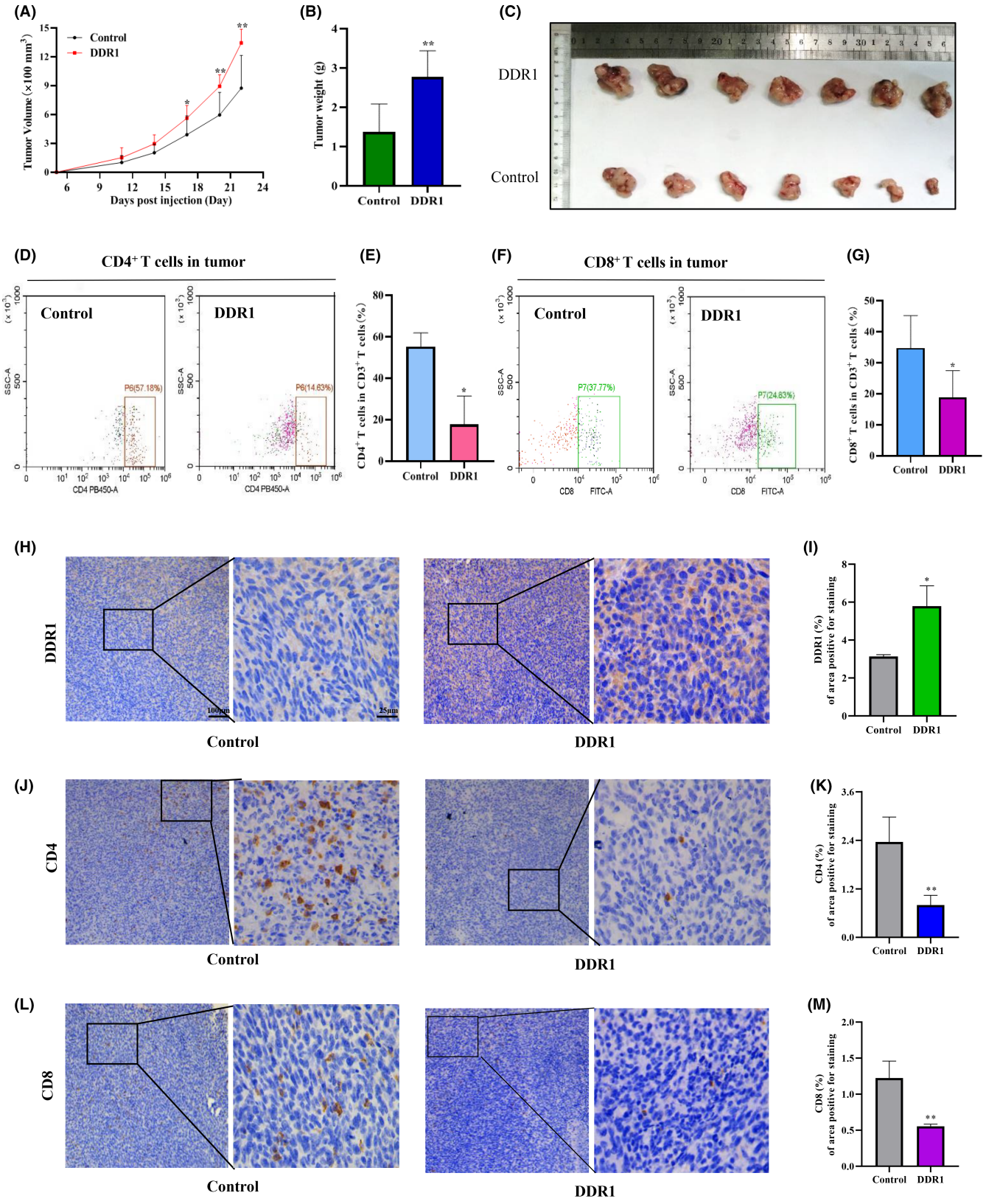

FIGURE 2 DDR1 overexpression inhibits the infiltration of immune cells in tumors. (A) Scramble control or DDR1-OE MC38 cells were injected subcutaneously into C57BL/6 mice ($n = 7$/group) and tumor size was measured. (B, C) After 22 days, the animals were sacrificed, and tumors were excised and weighed. DDR1-OE cells formed much bigger tumors. (D–G) Ratios of $CD4^+$ in $CD3^+$ lymphocytes and $CD8^+$ in $CD3^+$ lymphocytes in the two groups were compared as percentages. (H–M) Mouse tumor tissues from two groups (four out of seven samples were chosen randomly per group) were immunostained for DDR1, CD4, and CD8a. Scale, ×100 (left) and ×400 (right). Percentages of positive cells were measured using ImageJ software. Data are expressed as mean ± SD, $^*p < 0.05$; $^{**}p < 0.01$ (*t*-test).

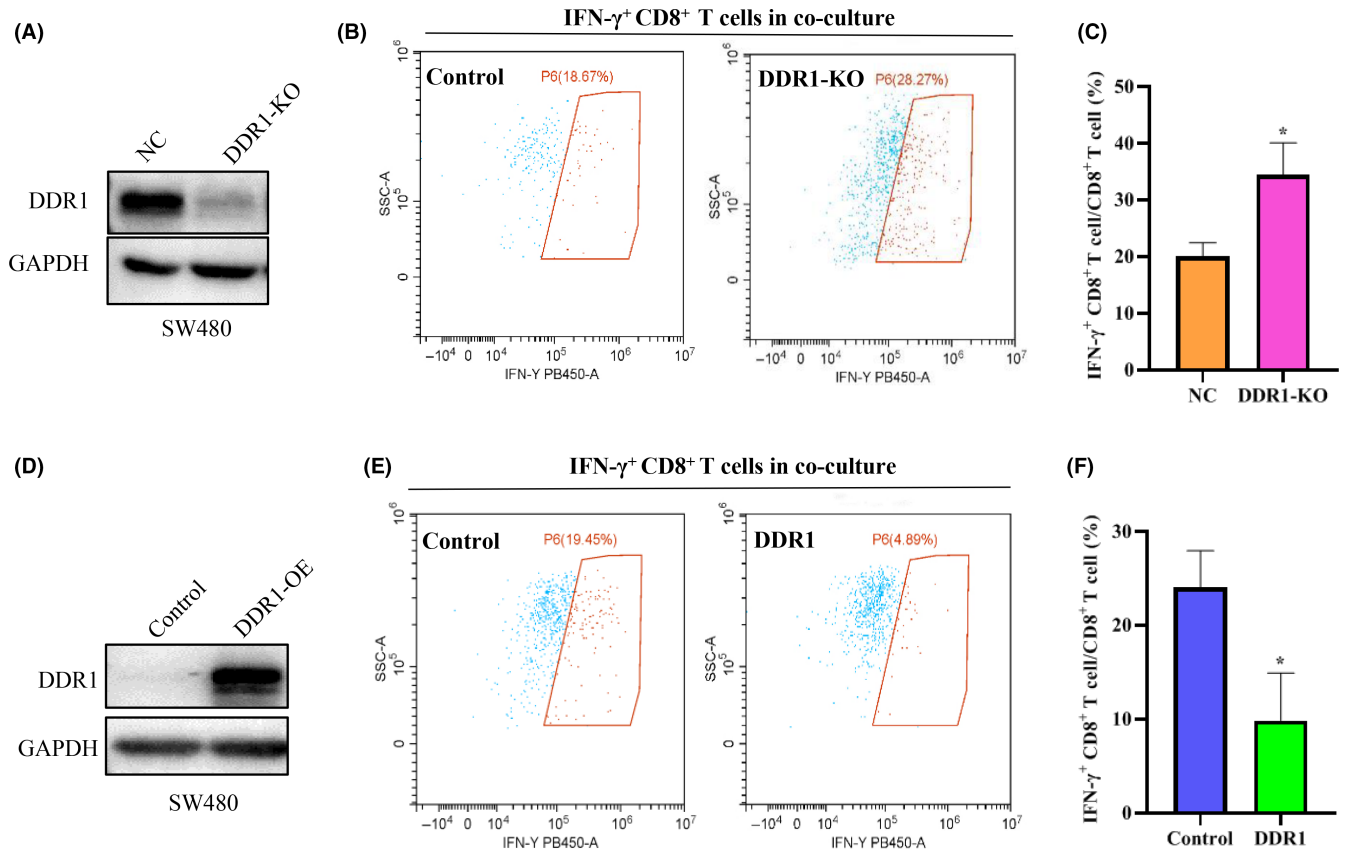

FIGURE 3 DDR1 affects $CD8^+$ T cell function co-cultured with CRC cells in vitro. (A) The DDR1-KO cell line was established. (B, C) DDR1-KO SW480 cells promoted the ratios of $CD8^+$ IFN-γ^+ T cells. (D) DDR1-OE in SW480 cells was verified. (E, F) DDR1-OE SW480 cells reduced the ratios of $CD8^+$ IFN-γ^+ T cells. Data are expressed as the mean ± SD of three independent experiments. *$p < 0.005$ (*t*-test).

cytokines, IL-18 was attractive as it functions as an immunomodulatory factor, inducing IFN-γ from natural killer (NK) cells and T cells in tumor foci.[19–23] Essentially, to convince the regulation of IL-18 by DDR1, we examined the IL-18 levels both in vivo and in vitro. We first confirmed that IL-18 levels were reduced in DDR1-OE tumor tissues by western blot and qRT-PCR (Figure 4A,B). Then we examined the level of IL-18 in DDR1-KO SW480 cells using western blot, qRT-PCR and ELISA, respectively, and showed that DDR1-KO promoted the synthesis and secretion of IL-18 (Figure 4C–E). Consistently, DDR1 knockdown profoundly provoked the synthesis and release of IL-18 (Figure 4F–H), whereas DDR1 overexpression induced a decreased IL-18 level in SW480 and HCT116 cells (Figure 4I–K). Overall, these results revealed that DDR1 regulated IL-18 synthesis and secretion in CRC, which may contribute to the sequestration of immune cells and the release of other crucial immune factors.

3.5 | DDR1 suppresses the infiltration and activation of T cells through inhibiting IL-18

To identify whether DDR1 regulates the activation of T cells through IL-18, we first overexpressed IL-18 in DDR1-OE SW480 cells (Figure 5A). Consistent with our hypothesis, the FCM showed that the IFN-γ level was elevated in the co-culture system, when IL-18 was added back in DDR1-overexpressed cells (Figure 5B,C). We then knocked down IL-18 with siRNA in DDR1-KO SW480 cells (Figure 5D). As expected, IL-18 knockdown in DDR1-depleted cells further decreased IFN-γ secretion from $CD8^+$ T cells in the co-culture system (Figure 5E,F). Furthermore, we exogenously changed the concentration of IL-18 in the co-culture system. rIL-18 (100 ng/ml) stimulated $CD8^+$ T cells to secret IFN-γ robustly when co-cultured with DDR1-OE SW480 cells (Figure 5G,H). By contrast, IL-18 neutralizing antibody (20 μg/ml) inhibited $CD8^+$ T cells to secret IFN-γ when co-cultured with DDR1-KO SW480 cells (Figure 5I,J). Therefore, IL-18 is one of the major downstream components through which DDR1 inhibits the activation of $CD8^+$ T cells in the co-culture system in vitro.

To explore the functional interaction between DDR1 and IL-18 in vivo, we overexpressed IL-18 in DDR1-OE MC38 cells (Figure 6A). MC38 cells bearing DDR1-OE + IL-18-OE formed much smaller tumors compared with DDR1-OE cells (Figure 6B–D). FCM analysis revealed a significant increase in $CD4^+$ and $CD8^+$ T cells in IL-18-OE + DDR1-OE tumors compared with DDR1-OE tumors (Figure 6E–H). Together, these findings suggested that IL-18-OE attenuates the immunosuppression and tumor growth of DDR1-OE and enhances the antitumor immune response in CRC.

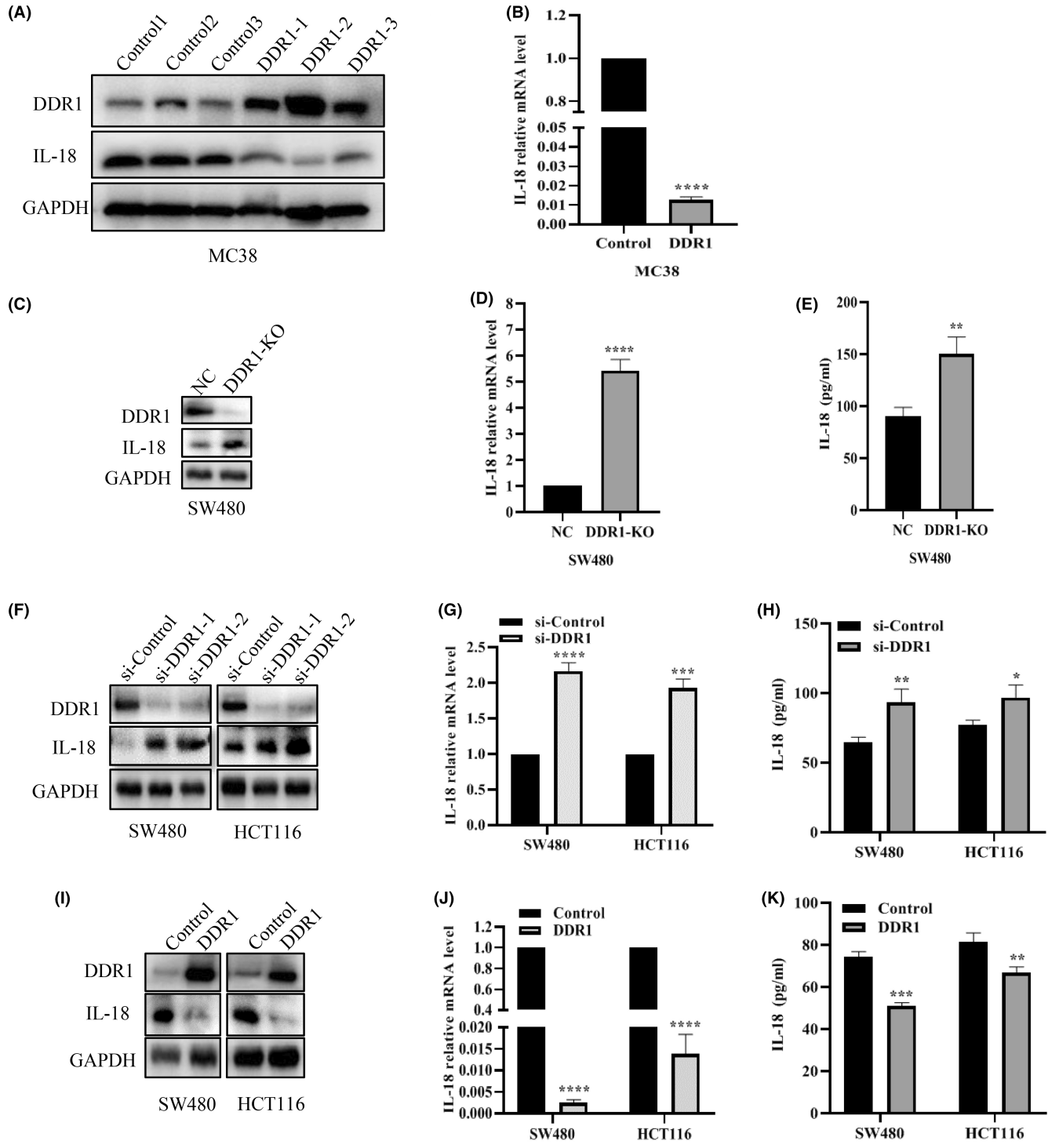

FIGURE 4 DDR1 affects the synthesis level of IL-18. (A, B) DDR1-OE reduced the mRNA and protein levels of IL-18 in tumor tissues. (C, D) DDR1-KO in SW480 increased the synthesis of IL-18 examined by western blot and qRT-PCR. (E) IL-18 secretion was evaluated by ELISA. (F–H) The deletion of DDR1 in HCT116 and SW480 cells increased the synthesis and release of IL-18. (I–K) DDR1 overexpression in cells decreased the synthesis and release of IL-18. Data are expressed as the mean ± SD of three independent experiments. *$p < 0.0.05$; **$p < 0.01$; ***$p < 0.001$;****$p < 0.0001$ (*t*-test).

FIGURE 5 IL-18 promotes $CD8^+$ T cell activation in co-culture. (A) A DDR1-OE + IL-18-OE SW480 cell line was established. (B, C) FCM analysis shows the proportion of IFN-γ^+CD8^+ T cells when $CD8^+$ T cells were co-cultured with DDR1-OE or DDR1-OE + IL-18-OE SW480 cells. (D) A DDR1-KO + IL-18-KD SW480 cell line was established. (E, F) FCM analysis shows the proportion of IFN-γ^+CD8^+ T cells when $CD8^+$ T cells were co-cultured with DDR1-KO or DDR1-KO + IL-18-KD SW480 cells. (G, H) FCM analysis shows the proportion of IFN-γ^+CD8^+ T cells after adding rIL-18 (100 ng/ml) or PBS including 5% trehalose in DDR1-OE co-culture. (I, J) FCM analysis shows the proportion of IFN-γ^+CD8^+ T cells after adding IL-18 neutralizing antibody (20 μg/ml) or control IgG in DDR1-KO co-culture. Data are expressed as the mean ± SD of three independent experiments. *$p < 0.05$; **$p < 0.01$; ****$p < 0.0001$ (*t*-test).

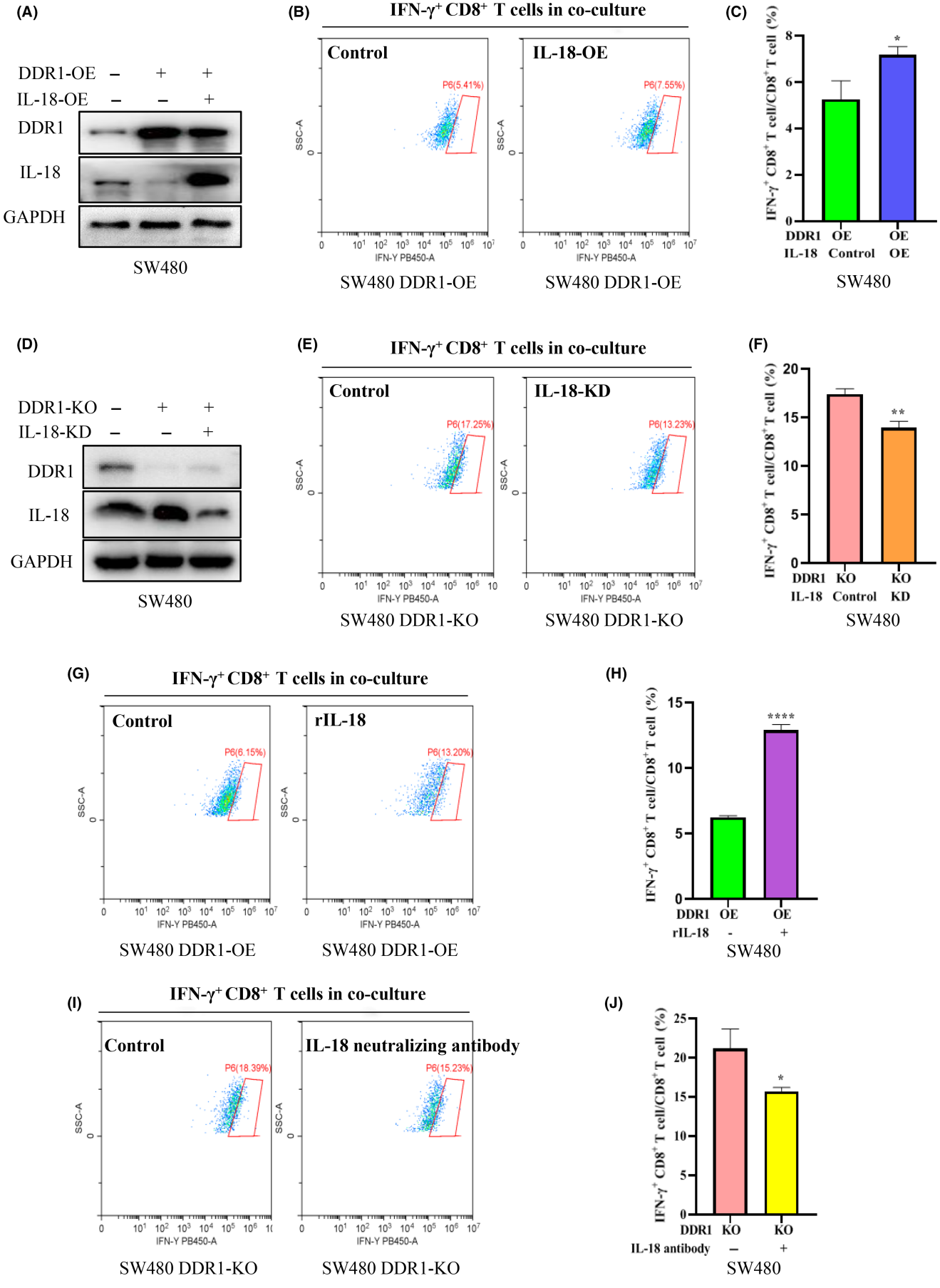
(A)
DDR1-OE – + +
IL-18-OE – – +
DDR1
IL-18
GAPDH
SW480
(B)
IFN-γ+ CD8+ T cells in co-culture
Control
P6(5.41%)
IL-18-OE
P6(7.55%)
SSC-A
IFN-Y PB450-A
SW480 DDR1-OE
SW480 DDR1-OE
(C)
IFN-γ+ CD8+ T cell/CD8+ T cell (%)
DDR1 OE OE
IL-18 Control OE
SW480
(D)
DDR1-KO – + +
IL-18-KD – – +
DDR1
IL-18
GAPDH
SW480
(E)
IFN-γ+ CD8+ T cells in co-culture
Control
P6(17.25%)
IL-18-KD
P6(13.23%)
SW480 DDR1-KO
SW480 DDR1-KO
(F)
IFN-γ+ CD8+ T cell/CD8+ T cell (%)
DDR1 KO KO
IL-18 Control KD
SW480
(G)
IFN-γ+ CD8+ T cells in co-culture
Control
P6(6.15%)
rIL-18
P6(13.20%)
SW480 DDR1-OE
SW480 DDR1-OE
(H)
IFN-γ+ CD8+ T cell/CD8+ T cell (%)
DDR1 OE OE
rIL-18 - +
SW480
(I)
IFN-γ+ CD8+ T cells in co-culture
Control
P6(18.39%)
IL-18 neutralizing antibody
P6(15.23%)
SW480 DDR1-KO
SW480 DDR1-KO
(J)
IFN-γ+ CD8+ T cell/CD8+ T cell (%)
DDR1 KO KO
IL-18 antibody – +
SW480

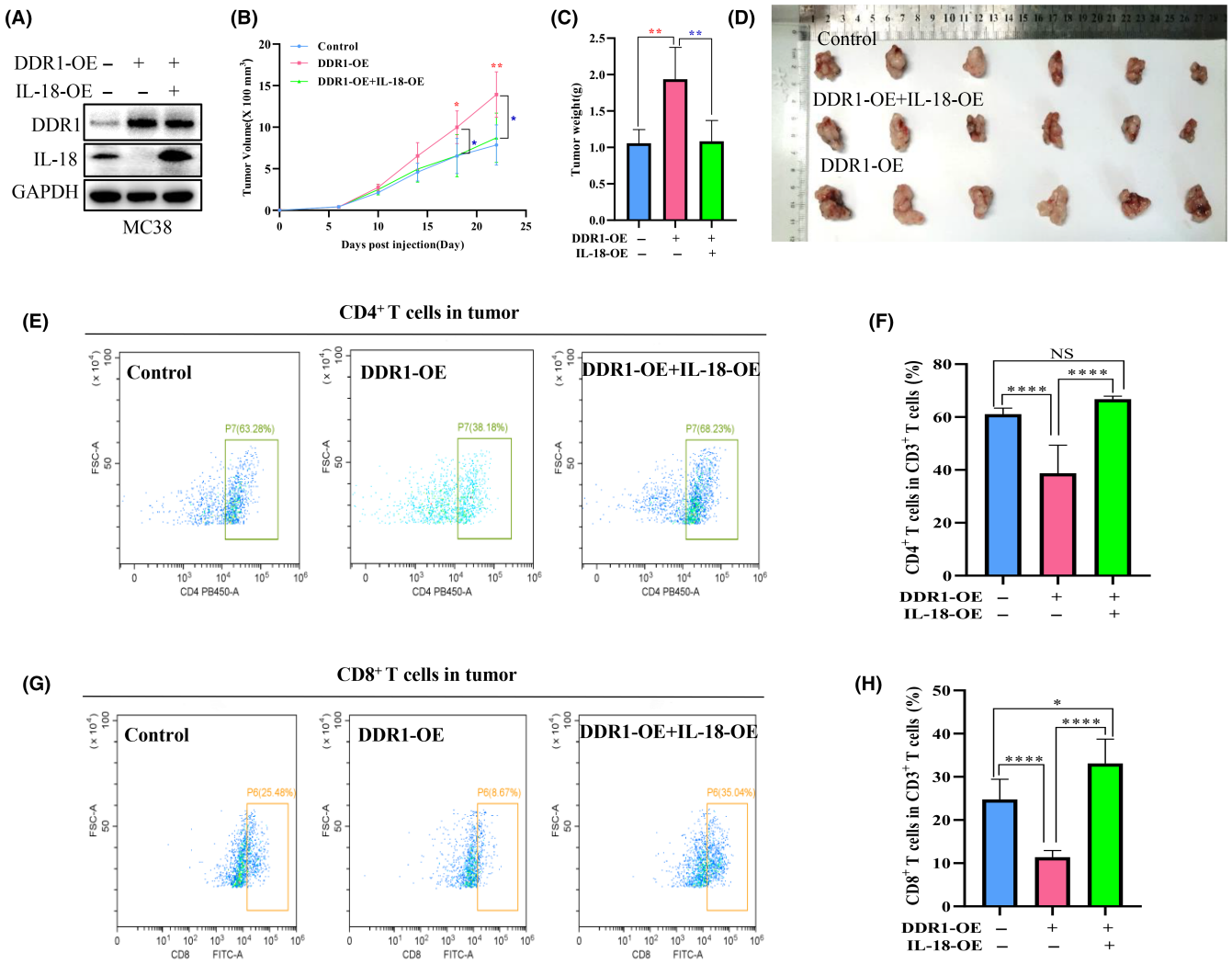

FIGURE 6 IL-18 overexpression promotes the infiltration of $CD4^+$ and $CD8^+$ T cells in tumor tissues. (A) A DDR1-OE + IL-18-OE MC38 cell line was established. (B–D) Scramble control, DDR1-OE and DDR1-OE + IL-18-OE MC38 cells were injected subcutaneously into C57BL/6 mice ($n = 6$/group). Tumor growth curves were plotted and all tumors (at the endpoint) were weighed and pictured. A red asterisk indicates the comparisons between control and DDR1-OE groups; blue asterisks indicated the comparisons between DDR1-OE and DDR1-OE + IL-18-OE groups. (E–H) FCM analyzed the proportion of $CD4^+$ and $CD8^+$ T cells from tumors in the scramble control, DDR1-OE and DDR1-OE + IL-18-OE groups ($n = 6$/group). Data are expressed as the mean ± SD. $^*p < 0.05$; $^{**}p < 0.01$; $^{****}p < 0.0001$ (one-way ANOVA followed by Tukey's multiple comparison test).

3.6 | DDR1 upregulates the expression of PD-L1

Binding between PD-L1 on cancer cells and PD-1 on TILs results in the suppression of the T cell receptor (TCR) pathway and the inhibition of T cell activity.[24–26] PD-L1 expression plays an important role in tumor immune escape. Therefore, we analyzed whether PD-L1 was regulated by DDR1 in our mouse model. PD-1 and PD-L1 staining were much higher in the DDR1-OE tumors than in the scramble controls (Figure 7A–D). Then, we examined PD-L1 expression using a western blot assay and found that PD-L1 was markedly elevated in DDR1-OE tumor tissues (Figure 7E). Accordingly, PD-L1 protein levels were decreased in DDR1-KD and DDR1-KO cells (Figure 7F). Consistently, DDR1 promoted PD-L1 expression in DDR1-OE cells (Figure 7G,H). Many studies have discussed the mechanisms regulating PD-L1

FIGURE 7 DDR1 upregulates the expression of PD-L1. (A–D) Mouse tumor tissues from two groups (four of seven were chosen at random per group) were immunostained for PD-1 and PD-L1. Scale, ×100 (left) and ×400 (right). Percentages of positive cells were measured using ImageJ software. (E) The indicated proteins in tumor tissues were analyzed by western blot. (F, G) The levels of indicated proteins were examined in DDR1 silencing cells as well as in DDR1-overexpressing cells. (H–J) The expression levels of PD-L1, KRAS and VEGFA were measured by qRT-PCR in DDR1-OE cells (SW480, HCT8, and RKO). (K) Control and DDR1-OE cells were treated with JNK inhibitor (10 μM) for 24 h and then the expression levels of p-JNK, PD-L1, and IL-18 were measured. Data are expressed as the mean ± SD of three independent experiments. $^*p < 0.05$; $^{**}p < 0.01$; $^{***}p < 0.001$; $^{****}p < 0.0001$ (*t*-test).

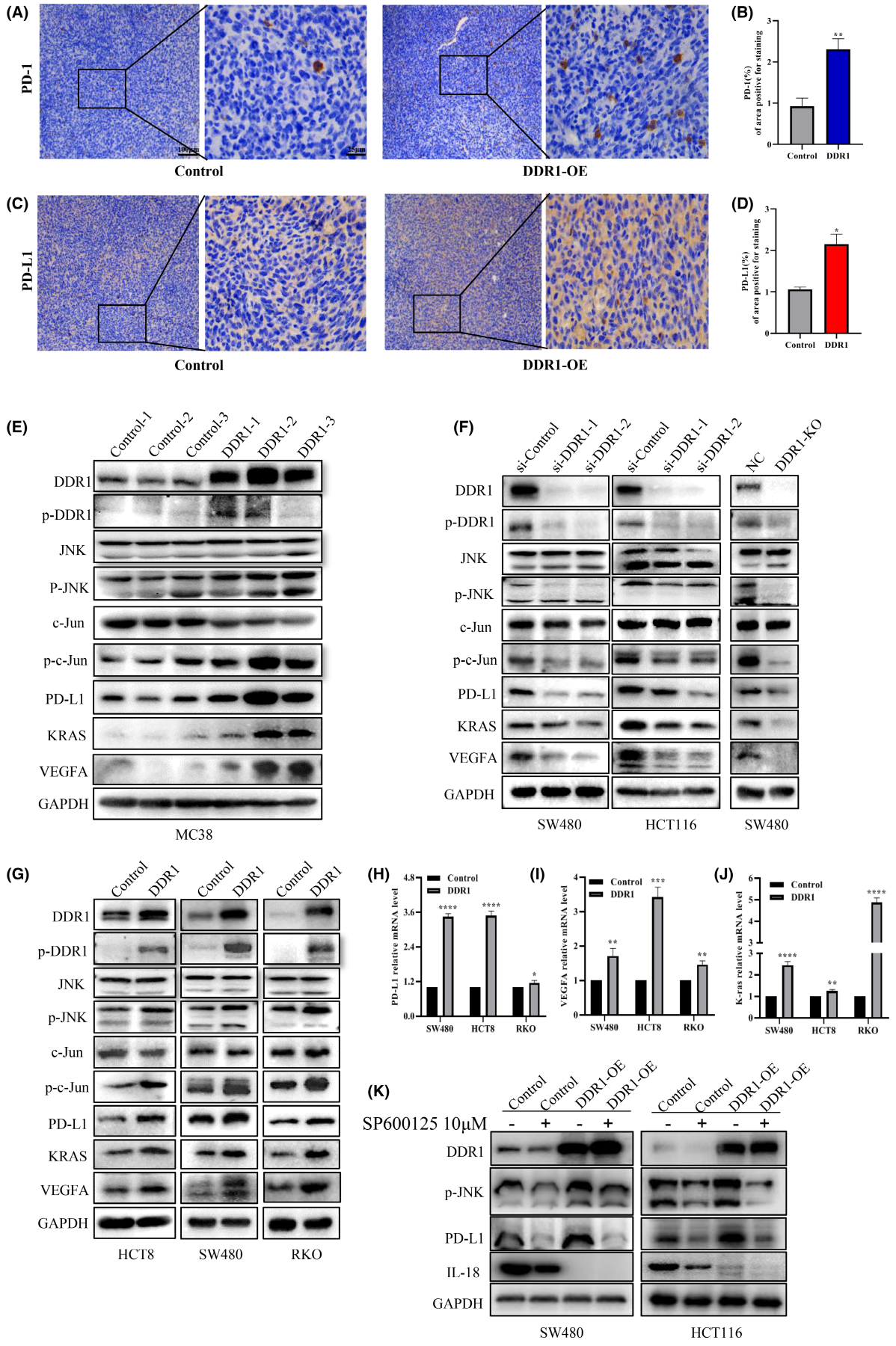
(A)
PD-1
Control
DDR1-OE
(B)
PD-1(%) of area positive for staining
Control
DDR1
(C)
PD-L1
Control
DDR1-OE
(D)
PD-L1(%) of area positive for staining
Control
DDR1
(E)
Control-1
Control-2
Control-3
DDR1-1
DDR1-2
DDR1-3
DDR1
p-DDR1
JNK
P-JNK
c-Jun
p-c-Jun
PD-L1
KRAS
VEGFA
GAPDH
MC38
(F)
si-Control
si-DDR1-1
si-DDR1-2
si-Control
si-DDR1-1
si-DDR1-2
NC
DDR1-KO
DDR1
p-DDR1
JNK
p-JNK
c-Jun
p-c-Jun
PD-L1
KRAS
VEGFA
GAPDH
SW480
HCT116
SW480
(G)
Control
DDR1
Control
DDR1
Control
DDR1
DDR1
p-DDR1
JNK
p-JNK
c-Jun
p-c-Jun
PD-L1
KRAS
VEGFA
GAPDH
HCT8
SW480
RKO
(H)
Control
DDR1
PD-L1 relative mRNA level
SW480
HCT8
RKO
(I)
Control
DDR1
VEGFA relative mRNA level
SW480
HCT8
RKO
(J)
Control
DDR1
K-ras relative mRNA level
SW480
HCT8
RKO
(K)
Control
Control
DDR1-OE
DDR1-OE
Control
Control
DDR1-OE
DDR1-OE
SP600125 10μM
- + - + - + - +
DDR1
p-JNK
PD-L1
IL-18
GAPDH
SW480
HCT116

expression.[27] Based on the available studies, we explored several pathways (JAK/STAT pathway, JNK/SAPK pathway, PI3K/AKT/mTOR pathway, and epidermal growth factor receptor [EGFR] pathway) in cells (Figure S4) that are possibly responsible for PD-L1 regulation. The phosphorylated protein levels of JNK signaling including p-JNK (Thr183/Tyr185) and p-c-Jun (Ser73) were increased in DDR1-OE mouse tumor tissues (Figure 7E). Consistent results were obtained in cells (Figure 7F,G). Previous studies showed that JNK/c-Jun signaling activation could significantly increase PD-L1 expression, and that the activation of c-Jun rendered promoters and enhancers of PD-L1 accessible.[28–30] To further clarify the mechanism, we used JNK inhibitor, SP600125 (10 μM), to suppress the phosphorylation of JNK for 24 h (Figure 7K). We observed the reduction of PD-L1 in both SW480 and HCT116 cells (Figure 7K). Therefore, DDR1 may upregulate PD-L1 expression at least partially through the JNK/c-Jun pathway. We also explored the role of IL-18 in the regulation of PD-L1, VEGFA, and KRAS expression. These did not vary significantly under various IL-18 expression levels (Figure S5).

Recently, accumulating evidence has shown that vascular endothelial growth factor A (VEGFA) significantly upregulated the expression of inhibitory immune checkpoints that mediated the exhaustion of intratumoral $CD8^+$ T cells.[31,32] We found that DDR1 was positively correlated with the expression of VEGFA in TCGA database (Figure S6A). Then we checked the expression of VEGFA in tumor tissues and cells (Figure 7E–G,I) and revealed that DDR1 enhanced VEGFA expression. In conclusion, we found that DDR1 upregulated PD-L1 expression through the JNK/c-Jun axis. In addition, DDR1 also regulated VEGFA expression, which may promoted $CD8^+$ T cell exhaustion. Interestingly, we found a positive correlation between DDR1 and KRAS in TCGA database (Figure S6B) and verified that DDR1 promotes KRAS expression at both the protein and mRNA levels (Figure 7E–G,J). The specific mechanism remains to be further explored.

4 | DISCUSSION

It is known that the accumulation of tumor-specific $CD4^+$ and $CD8^+$ T cells is critical for an effective antitumor response.[33] Here, we provide evidence that DDR1 is a major regulator controlling the infiltration of $CD4^+$ and $CD8^+$ T cells in CRC (Figure S7). Our study revealed that the infiltration of immune killer cells was decreased in DDR1-OE tumors, suggesting that DDR1 could promote the formation of immunosuppressive microenvironments in CRC. $CD4^+$ T cells promote the recruitment and effector function of tumor-specific $CD8^+$ T cells and activate innate killer cells in the tumor.[34,35] Furthermore, IFN-γ exerts direct antiproliferative and proapoptotic antitumor effects.[36,37] We found that DDR1 is also responsible for the activity of $CD8^+$ cells through inhibiting the synthesis of IFN-γ in CRC.

For the mechanism of DDR1 in regulating immunity, we found that IL-18 was changed significantly upon DDR1 inhibition or overexpression. Early studies have shown that IL-18 can induce the production of IFN-γ and stressed its role as an inducer of Th1 responses.[23] Recently, it was demonstrated that IL-18 promoted the expansion and survival of effector cells including NK and $CD8^+$ T cells that expressed IL-18 receptor α/β chains and receptors containing an immunoreceptor tyrosine-based activation motif (ITAM).[38,39] IL-18 performs its biological functions by ligation of IL-18 receptors (IL-18R) α and β, and activates $CD4^+$, $CD8^+$ T, and NK cells through NF-κB activation, leading to IFN-γ production in target cells.[21,40] Therapeutically, immune checkpoint inhibitors and IL-18 synergistically inhibited the growth of tumor cells without significant adverse events in animal models.[41] A phase II study of recombinant IL-18 (rIL-18) was conducted in an untreated American Joint Committee on Cancer (AJCC) stage IV melanoma and rIL-18, tested in this trial, was well tolerated.[42] These results highlighted the potential of the IL-18 pathway for immunotherapeutic intervention.

The effect of DDR1 on T cell exhaustion should also be concerned. Exhausted $CD8^+$ T cells in cancer frequently express high level of inhibitory receptors, including PD-1, CTLA-4, LAG-3, and so forth.[43–45] Our study found that the DDR1-OE tumors had stronger PD-1/PD-L1 staining, which may result in an immunosuppressive microenvironment. VEGFA is not only an important driver of tumor angiogenesis, but also an important suppressive factor of antitumor immunity.[46–48] Our study highlighted that DDR1 can regulate VEGFA expression, but also raised complex questions. For example, how does DDR1 regulate VEGFA? And what role does VEGFA play in T cell immersion upon DDR1 inhibition? Many studies have reported the regulatory mechanisms of PD-L1 expression,[27] but the role of DDR1 in this has not been examined. We found that DDR1 regulates the activity of JNK/c-Jun pathway, which is essential for the expression level of PD-L1 (Figure S7). Knockdown of JNK or treatment with the JNK inhibitor, SP600125, led to reduced PD-L1 expression.[49,50] Mechanistically, DDR1 phosphorylation induced the phosphorylation and the nuclear localization of c-Jun by activating JNK, and then promoted the transcription of PD-L1.[30,51–53] Therefore, whether the combination of anti-PD-1/PD-L1 antibodies, antiangiogenic therapy, and DDR1 inhibitor will have synergetic effects in CRC needs to be further explored, and may contribute a way in which to solve the limited application of immunotherapy.[54]

We also found that DDR1 was positively correlated with the expression of KRAS. Several studies have confirmed that DDR1 can improve the efficacy of KRAS-mutant tumors.[55–57] For example, combining DDR1 inhibition with chemotherapy prompted a synergistic therapeutic effect and enhanced the cell death of KRAS-mutant tumors in vivo.[57] It was also reported that the combined inhibition of DDR1 and Notch signaling could be an effective targeted therapy for patients with KRAS-mutant lung adenocarcinoma.[55] However, how DDR1 regulates KRAS expression and whether DDR1 improves the efficacy of immunotherapy in CRC patients with KRAS mutations require further investigation.

Recently, Sun et al.[58] reported the role of DDR1 in immunity in triple-negative breast cancer (TNBC), which is consistent with our results. They also showed that DDR1 instigates immune exclusion by promoting collagen fiber alignment, which is an inspiring progress.[58] In our study, we demonstrated that DDR1 plays a vital role in

tumor growth in vivo through regulating immune cell infiltration in CRC. The immune-regulatory function of DDR1 is at least partially mediated by IL-18, VEGFA, and PD-L1 expression. Therefore, targeting DDR1 may represent a new strategy to enhance the efficacy of immunotherapy, which provides a direction to convert current challenges into opportunities.

AUTHOR CONTRIBUTIONS

Xiaofan Duan and Xiaoxiao Xu designed the research and performed experiments; Yumei Zhang contributed to animal experiments of article revision. Yuan Gao contributed to data visualization. Xiaofan Duan and Xiaoxiao Xu wrote the original draft; Jin Li and Jiuli Zhou designed the research, supervised the study, and revised the manuscript. The work reported in this paper has been performed by the authors, unless clearly specified in the text.

ACKNOWLEDGMENTS

We thank Professor Qiang Ma (Southern Medical University, China) for the mouse cell line MC38.

FUNDING INFORMATION

This work was supported by the Top-level Clinical Discipline Project of Shanghai Pudong (PWYgf2021-07), National Natural Science Foundation of China (81772561) and the Shanghai Sailing Program (20YF1453300).

DISCLOSURE

All authors declare that they have no conflict of interest. Jin Li, the corresponding author for this study, is the Associate Editor of Cancer Science.

ETHICAL APPROVAL

Approval of the research protocol by an Institutional Reviewer Board: The research protocol was approved by the Ethics Committee of Shanghai East Hospital (EC.D [BG]0.016.02.1) and it conformed to the provisions of the Declaration of Helsinki.

Informed consent: Informed consent was obtained from healthy donors.

Registry and the registration no. of the study/trial: N/A.

Animal studies: All animal experiments were approved by the Animal Care and Use Committee of laboratory animal research center, Tongji University (TJBB04521101).

ORCID

Xiaofan Duan https://orcid.org/0000-0001-6231-9357
Yumei Zhang https://orcid.org/0000-0002-3261-2277
Yuan Gao https://orcid.org/0000-0003-3227-2310
Jin Li https://orcid.org/0000-0001-5523-0055

REFERENCES

1. Keum N, Giovannucci E. Global burden of colorectal cancer: emerging trends, risk factors and prevention strategies. *Nat Rev Gastroenterol Hepatol*. 2019;16:713-732.
2. Galon J, Costes A, Sanchez-Cabo F, et al. Type, density, and location of immune cells within human colorectal tumors predict clinical outcome. *Science*. 2006;313:1960-1964.
3. Ganesh K, Stadler ZK, Cercek A, et al. Immunotherapy in colorectal cancer: rationale, challenges and potential. *Nat Rev Gastroenterol Hepatol*. 2019;16:361-375.
4. Pagès F, Mlecnik B, Marliot F, et al. International validation of the consensus immunoscore for the classification of colon cancer: a prognostic and accuracy study. *Lancet*. 2018;391:2128-2139.
5. Galon J, Bruni D. Approaches to treat immune hot, altered and cold tumours with combination immunotherapies. *Nat Rev Drug Discov*. 2019;18:197-218.
6. Galon J, Fridman WH, Pages F. The adaptive immunologic microenvironment in colorectal cancer: a novel perspective. *Cancer Res*. 2007;67:1883-1886.
7. Moll S, Desmouliere A, Moeller MJ, et al. DDR1 role in fibrosis and its pharmacological targeting. *Biochim Biophys Acta Mol Cell Res*. 2019;1866:118474.
8. Leitinger B. Discoidin domain receptor functions in physiological and pathological conditions. *Int Rev Cell Mol Biol*. 2014;310:39-87.
9. Rammal H, Saby C, Magnien K, et al. Discoidin domain receptors: potential actors and targets in cancer. *Front Pharmacol*. 2016;7:55.
10. Gao Y, Zhou J, Li J. Discoidin domain receptors orchestrate cancer progression: a focus on cancer therapies. *Cancer Sci*. 2021;112:962-969.
11. Jeitany M, Leroy C, Tosti P, et al. Inhibition of DDR1-BCR signalling by nilotinib as a new therapeutic strategy for metastatic colorectal cancer. *EMBO Mol Med*. 2018;10:e7918.
12. Le CC, Bennasroune A, Collin G, et al. LRP-1 promotes colon cancer cell proliferation in 3D collagen matrices by mediating DDR1 endocytosis. *Front Cell Dev Biol*. 2020;8:412.
13. He Y, Hara H, Nunez G. Mechanism and regulation of NLRP3 inflammasome activation. *Trends Biochem Sci*. 2016;41:1012-1021.
14. Swanson KV, Deng M, Ting JP. The NLRP3 inflammasome: molecular activation and regulation to therapeutics. *Nat Rev Immunol*. 2019;19:477-489.
15. Kinoshita M, Seki S, Ono S, Shinomiya N, Hiraide H. Paradoxical effect of IL-18 therapy on the severe and mild *Escherichia coli* infections in burn-injured mice. *Ann Surg*. 2004;240:313-320.
16. Farhood B, Najafi M, Mortezaee K. CD8(+) cytotoxic T lymphocytes in cancer immunotherapy: a review. *J Cell Physiol*. 2019;234:8509-8521.
17. Briukhovetska D, Dörr J, Endres S, Libby P, Dinarello CA, Kobold S. Interleukins in cancer: from biology to therapy. *Nat Rev Cancer*. 2021;21:481-499.
18. Li J, Huang L, Zhao H, Yan Y, Lu J. The role of interleukins in colorectal cancer. *Int J Biol Sci*. 2020;16:2323-2339.
19. Zhou T, Damsky W, Weizman OE, et al. IL-18BP is a secreted immune checkpoint and barrier to IL-18 immunotherapy. *Nature*. 2020;583:609-614.
20. Esmailbeig M, Ghaderi A. Interleukin-18: a regulator of cancer and autoimmune diseases. *Eur Cytokine Netw*. 2017;28:127-140.
21. Li Z, Yu X, Werner J, Bazhin AV, D'Haese JG. The role of interleukin-18 in pancreatitis and pancreatic cancer. *Cytokine Growth Factor Rev*. 2019;50:1-12.
22. Nakamura K, Bald T, Smyth MJ. Cancer-killing, decoy-resistant interleukin-18. *Immunol Cell Biol*. 2020;98:434-436.
23. Dinarello CA, Kaplanski G. Indeed, IL-18 is more than an inducer of IFN-gamma. *J Leukoc Biol*. 2018;104:237-238.
24. Schildberg FA, Klein SR, Freeman GJ, Sharpe AH. Coinhibitory pathways in the B7-CD28 ligand-receptor family. *Immunity*. 2016;44:955-972.
25. Kim HD, Song GW, Park S, et al. Association between expression level of PD1 by tumor-infiltrating CD8(+) T cells and features of hepatocellular carcinoma. *Gastroenterology*. 2018;155:1936-1950.e17.

26. Wang X, He Q, Shen H, et al. TOX promotes the exhaustion of antitumor CD8(+) T cells by preventing PD1 degradation in hepatocellular carcinoma. *J Hepatol*. 2019;71:731-741.
27. Cha JH, Chan LC, Li CW, Hsu JL, Hung MC. Mechanisms controlling PD-L1 expression in cancer. *Mol Cell*. 2019;76:359-370.
28. Cui L, Chen SY, Lerbs T, et al. Activation of JUN in fibroblasts promotes pro-fibrotic programme and modulates protective immunity. *Nat Commun*. 2020;11:2795.
29. Shang A, Wang W, Gu C, et al. Long non-coding RNA HOTTIP enhances IL-6 expression to potentiate immune escape of ovarian cancer cells by upregulating the expression of PD-L1 in neutrophils. *J Exp Clin Cancer Res*. 2019;38:411.
30. Wang H, Fu C, Du J, et al. Enhanced histone H3 acetylation of the PD-L1 promoter via the COP1/c-Jun/HDAC3 axis is required for PD-L1 expression in drug-resistant cancer cells. *J Exp Clin Cancer Res*. 2020;39:29.
31. Meder L, Schuldt P, Thelen M, et al. Combined VEGF and PD-L1 blockade displays synergistic treatment effects in an autochthonous mouse model of small cell lung cancer. *Cancer Res*. 2018;78:4270-4281.
32. Deng H, Kan A, Lyu N, et al. Dual vascular endothelial growth factor receptor and fibroblast growth factor receptor inhibition elicits antitumor immunity and enhances programmed cell Death-1 checkpoint blockade in hepatocellular carcinoma. *Liver Cancer*. 2020;9:338-357.
33. Kortekaas KE, Santegoets SJ, Sturm G, et al. CD39 identifies the CD4(+) tumor-specific T-cell population in human cancer. *Cancer Immunol Res*. 2020;8:1311-1321.
34. Borst J, Ahrends T, Babala N, Melief CJM, Kastenmuller W. CD4(+) T cell help in cancer immunology and immunotherapy. *Nat Rev Immunol*. 2018;18:635-647.
35. Zhang L, Yu X, Zheng L, et al. Lineage tracking reveals dynamic relationships of T cells in colorectal cancer. *Nature*. 2018;564:268-272.
36. Kursunel MA, Esendagli G. The untold story of IFN-gamma in cancer biology. *Cytokine Growth Factor Rev*. 2016;31:73-81.
37. Burke JD, Young HA. IFN-gamma: a cytokine at the right time, is in the right place. *Semin Immunol*. 2019;43:101280.
38. Li W, Kashiwamura S, Ueda H, Sekiyama A, Okamura H. Protection of CD8+ T cells from activation-induced cell death by IL-18. *J Leukoc Biol*. 2007;82:142-151.
39. Ortaldo JR, Young HA. IL-18 as critical co-stimulatory molecules in modulating the immune response of ITAM bearing lymphocytes. *Semin Immunol*. 2006;18:193-196.
40. Nakanishi K, Yoshimoto T, Tsutsui H, Okamura H. INTERLEUKIN-18 regulates both TH1 and TH2 responses. *Annu Rev Immunol*. 2001;19:423-474.
41. Ma Z, Li W, Yoshiya S, et al. Augmentation of immune checkpoint cancer immunotherapy with IL18. *Clin Cancer Res*. 2016;22:2969-2980.
42. Tarhini AA, Millward M, Mainwaring P, et al. A phase 2, randomized study of SB-485232, rhIL-18, in patients with previously untreated metastatic melanoma. *Cancer*. 2009;115:859-868.
43. Fourcade J, Sun Z, Benallaoua M, et al. Upregulation of Tim-3 and PD-1 expression is associated with tumor antigen-specific CD8+ T cell dysfunction in melanoma patients. *J Exp Med*. 2010;207:2175-2186.
44. Blackburn SD, Shin H, Haining WN, et al. Coregulation of CD8+ T cell exhaustion by multiple inhibitory receptors during chronic viral infection. *Nat Immunol*. 2009;10:29-37.
45. He QF, Xu Y, Li J, Huang ZM, Li XH, Wang X. CD8+ T-cell exhaustion in cancer: mechanisms and new area for cancer immunotherapy. *Brief Funct Genom*. 2019;18:99-106.
46. Fukumura D, Kloepper J, Amoozgar Z, Duda DG, Jain RK. Enhancing cancer immunotherapy using antiangiogenics: opportunities and challenges. *Nat Rev Clin Oncol*. 2018;15:325-340.
47. Lee WS, Yang H, Chon HJ, Kim C. Combination of anti-angiogenic therapy and immune checkpoint blockade normalizes vascular-immune crosstalk to potentiate cancer immunity. *Exp Mol Med*. 2020;52:1475-1485.
48. Kudo M. Scientific rationale for combined immunotherapy with PD-1/PD-L1 antibodies and VEGF inhibitors in advanced hepatocellular carcinoma. *Cancers (Basel)*. 2020;12:1089.
49. Liu J, Hamrouni A, Wolowiec D, et al. Plasma cells from multiple myeloma patients express B7-H1 (PD-L1) and increase expression after stimulation with IFN-{gamma} and TLR ligands via a MyD88-, TRAF6-, and MEK-dependent pathway. *Blood*. 2007;110:296-304.
50. Qian Y, Deng J, Geng L, et al. TLR4 signaling induces B7-H1 expression through MAPK pathways in bladder cancer cells. *Cancer Invest*. 2008;26:816-821.
51. Ma G, Liang Y, Chen Y, et al. Glutamine deprivation induces PD-L1 expression via activation of EGFR/ERK/c-Jun signaling in renal cancer. *Mol Cancer Res*. 2020;18:324-339.
52. Wang JJ, Siu MK, Jiang YX, et al. Aberrant upregulation of PDK1 in ovarian cancer cells impairs CD8(+) T cell function and survival through elevation of PD-L1. *Onco Targets Ther*. 2019;8:e1659092.
53. Chen Y-C, Huang M-Y, Zhang L-L, et al. Nagilactone E increases PD-L1 expression through activation of c-Jun in lung cancer cells. *Chin J Nat Med*. 2020;18:517-525.
54. Oliveira AF, Bretes L, Furtado I. Review of PD-1/PD-L1 inhibitors in metastatic dMMR/MSI-H colorectal cancer. *Front Oncol*. 2019;9:396.
55. Ambrogio C, Gomez-Lopez G, Falcone M, et al. Combined inhibition of DDR1 and notch signaling is a therapeutic strategy for KRAS-driven lung adenocarcinoma. *Nat Med*. 2016;22:270-277.
56. Ambrogio C, Nadal E, Villanueva A, et al. KRAS-driven lung adenocarcinoma: combined DDR1/notch inhibition as an effective therapy. *ESMO Open*. 2016;1:e000076.
57. Nokin MJ, Darbo E, Travert C, et al. Inhibition of DDR1 enhances in vivo chemosensitivity in KRAS-mutant lung adenocarcinoma. *JCI Insight*. 2020;5:e137869.
58. Sun X, Wu B, Chiang HC, et al. Tumour DDR1 promotes collagen fibre alignment to instigate immune exclusion. *Nature*. 2021;599:673-678.

SUPPORTING INFORMATION

Additional supporting information can be found online in the Supporting Information section at the end of this article.

How to cite this article: Duan X, Xu X, Zhang Y, Gao Y, Zhou J, Li J. DDR1 functions as an immune negative factor in colorectal cancer by regulating tumor-infiltrating T cells through IL-18. *Cancer Sci*. 2022;113:3672-3685. doi: 10.1111/cas.15533